Earth Planets Space, **51**, 593–610, 1999

Planetary scale and tidal perturbations in mesospheric temperature observed by WINDII

M. G. Shepherd[1], W. E. Ward[2], B. Prawirosoehardjo[1], R. G. Roble[3], S.-P. Zhang[1], and D. Y. Wang[2]

[1*]*Centre for Research in Earth and Space Science, York University, Toronto, Canada*
[2]*Centre for Research in Earth and Space Technology, Toronto, Canada*
[3]*High Altitude Observatory, National Center for Atmospheric Research, Boulder, CO, U.S.A.*

(Received August 11, 1998; Revised June 25, 1999; Accepted June 25, 1999)

WINDII, the Wind Imaging Interferometer on the Upper Atmospheric Research Satellite measures winds and emission rates from selected excited metastable species. Here we report on measurements of the atmospheric Rayleigh scattering from the O(^{1}S) background filter at 553 nm wavelength used to derive temperature profiles in the upper mesosphere from 70 km to 95 km, for solstice periods from December 1992/93 and January 1993/94. The data are first zonally averaged and then combined in local time over about one month. Based on these temperatures, an analysis of planetary wave structures and tidal perturbations employing least-mean-square (LMS) fits to the data has been conducted and the results are presented. The planetary wave structures observed were well described with a quasi two-day wave (QTDW). Amplitudes of 14 K and 10 K at 85 km height for downleg (descending) and upleg (ascending) sampling respectively at latitudes from 20°S to 40°S were found to be in good agreement with QTDW temperature results from the MLS/UARS experiment assuming a vertical amplitude structure of the type described by the HRDI/UARS mesospheric wind observations. It is shown that the diurnal tide amplitudes estimated from latitudes from 25°N to 35°S using the LMS fit maximize at the equator with an amplitude of about 6 K and decrease toward tropical latitudes, consistent with the classical tidal theory and predictions from the TIME-GCM model.

1. Introduction

The atmosphere between 80 and 100 km is one of the most difficult regions to study experimentally. The dominant source of temperature information for this region comes from rocket based in-situ measurements, ground-based lidar observations and in the last decade—from satellite missions like the SME (Clancy and Rush, 1989; Clancy *et al.*, 1994) and UARS (Reber *et al.*, 1993).

The most extensive observations of middle atmosphere thermal tides relied on ground-based optical techniques (Wiens *et al.*, 1995; Yu *et al.*, 1997; Hecht *et al.*, 1998; States and Gardner, 1998; von Zahn *et al.*, 1998). These data, although with high time resolution, are limited to a few geographical locations. On the other hand, satellites provide long term, continuous global coverage of the middle atmosphere, although with much coarser time resolution. Satellite studies successfully demonstrated the feasibility and methodology of obtaining global tidal analysis from sun-synchronous satellite measurements (i.e. Hitchman and Leovy, 1985; Lieberman, 1991).

While much effort has been devoted to the study and modeling of tidal perturbations and planetary waves in the mesosphere/lower thermosphere (MLT) wind field (i.e. Hays *et al.*, 1994; Burrage *et al.*, 1995; Hagan *et al.*, 1995, 1997; McLandress *et al.*, 1996; Akmaev *et al.*, 1997; Yudin *et al.*, 1997; Wang *et al.*, 1997, and references therein), few studies have addressed the dynamics of the temperature field in that region (i.e. Rodgers and Prata, 1981; Hitchman and Leovy, 1985; Dudhia *et al.*, 1993; Wu *et al.*, 1996; Ward *et al.*, 1998). Many of the published mesospheric temperature studies have been focused on the accuracy of the retrieved temperature profiles, and a determination of climatological means and trends.

In the following sections we present results from analysis of tidal perturbations and planetary scale waves, such as the quasi two-day wave, in mesospheric temperature data from the 70–95 km height range, from the Wind Imaging Interferometer (WINDII) (Shepherd *et al.*, 1993a) on UARS. These have been identified as major features in the analysis of the wind data of WINDII and HRDI on UARS and it is of interest to identify their form in the WINDII temperature data. The observed mean temperature field, tidal amplitudes and phases are compared with some model predictions by the TIME-GCM (Roble and Ridley, 1994), while the quasi two-day wave results are discussed in the context of the UARS/MLS (Wu *et al.*, 1996) temperature observations and the WINDII and HRDI wind signatures.

2. WINDII Temperature Data

The vertical temperature profiles are derived from Rayleigh scattering measurements by the WINDII background filter at 553 nm wavelength. The WINDII measurements are limb images of the MLT with tangent heights that range in average from 65 to 115 km above the surface in

*CRESS, York University, 4700 Keele Street, North York, Ont, Canada, M4J 1P3.

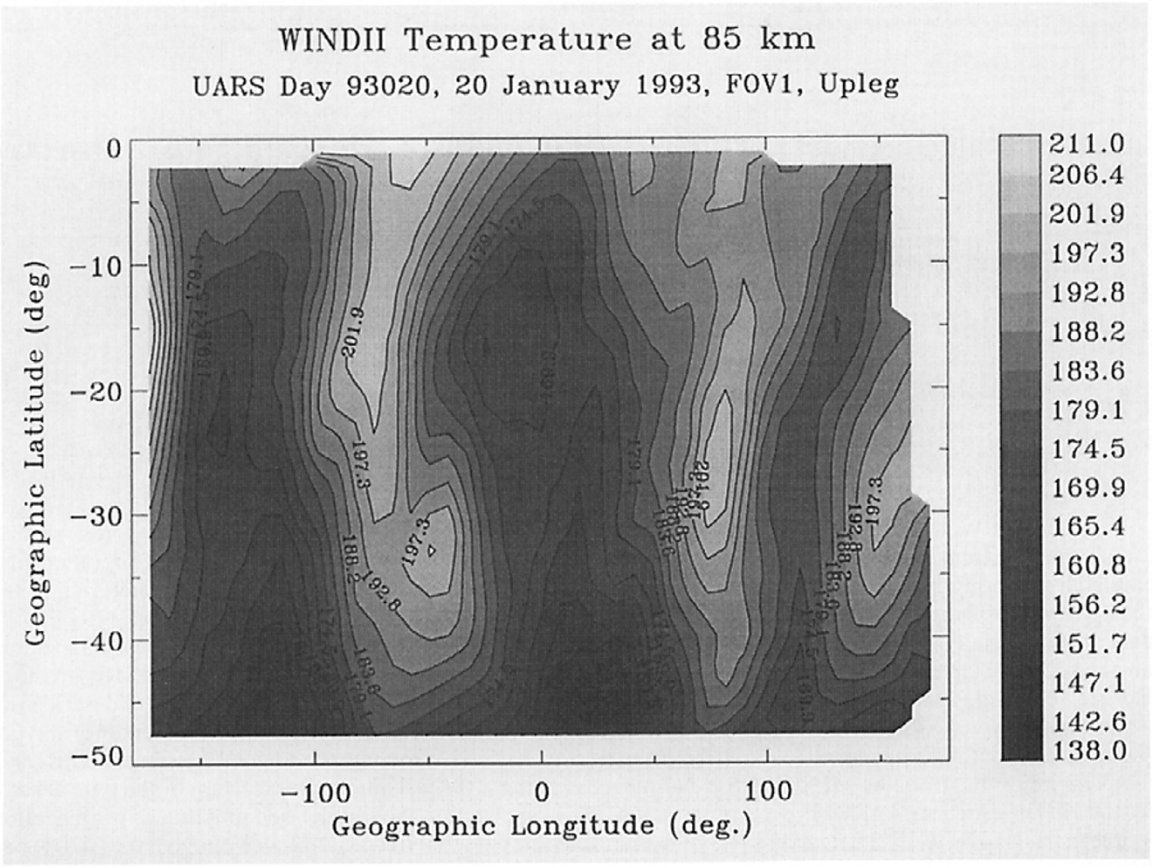

Fig. 1a. Map of the WINDII temperatures at 85 km, in the Southern hemisphere for January 20, 1993. The colour table units are for temperature in Kelvin (K).

2.2 km increments. The measurements sample horizontal segments of 25 km with 5 km bins and are integrated along the line-of-sight direction over a distance of roughly 400 km. The two look directions view at 45° and 135° from the UARS satellite track.

Due to the orbital inclination of the UARS spacecraft, the maximum latitude coverage observed is from about 72° in one hemisphere to 42° in the other. The viewing geometry of WINDII depends on the pointing direction of UARS which rotates 180° every 36 days. On a single day WINDII completes 15 orbits while the Earth rotates beneath it, thus providing a full longitudinal coverage over a given latitude circle. For an earth-bound observer, the observing points drift westward along a latitude circle at a rate of about 365° of longitude per day. This corresponds to a 20-minute change in the local time of each subsequent day's measurement. About 72 days are thus required for all solar times to be sampled by the satellite on a single node. However, since the orbit has both ascending and descending portions it takes only 36 days to cover the complete diurnal range. Under these conditions WINDII is able to provide data for tidal analysis by collecting observations over a month.

The temperature retrieval is based on an approach similar to that employed in the analysis of Rayleigh lidar data. Assuming that the atmosphere is in hydrodynamical equilibrium and is described by the ideal gas law, the temperature is derived from the atmospheric scale height at given altitude. In the case of WINDII the measurements are integral line-of-sight values of the Rayleigh scattering radiances, which are inverted to volume emission rates at the tangent height from which the derived temperature is assigned to that tangent height. The temperature inversion employs a Chahine-type routine (i.e. Chahine, 1977; Twomey, 1977) which will be discussed in detail in an upcoming paper. Some earlier results were discussed by Shepherd *et al.* (1997). Since the molecular scatter signal which is proportional to atmospheric density is very weak in the upper mesosphere the SNR and the measurement accuracy rapidly deteriorates with height at altitudes above about 95 km. Therefore, at present, meaningful temperature values can be derived only below about 90 km altitude.

Most of the results presented herein concern the analysis of temperatures for solstice conditions from December 24, 1992 to January 30, 1994. This period encompasses the 10-day campaign, January 19–January 30, 1993 designated for studies of the mesosphere-low-thermosphere (MLT) region and characterized in particular by studies of quasi-two-day wave (Wu *et al.*, 1993, Ward *et al.*, 1996). Although the local time (LT) sampling is less representative than that of the combined 1992/93 and 1993/94 December solstice datasets, starting with the 1992/93 data allows us to relate more directly the temperature results from the QTDW and diurnal tidal analysis, features previously identified in the analysis of wind data from the same period of time. A comparison with the analysis of the more general and complete 1992/94 data will also be presented and discussed.

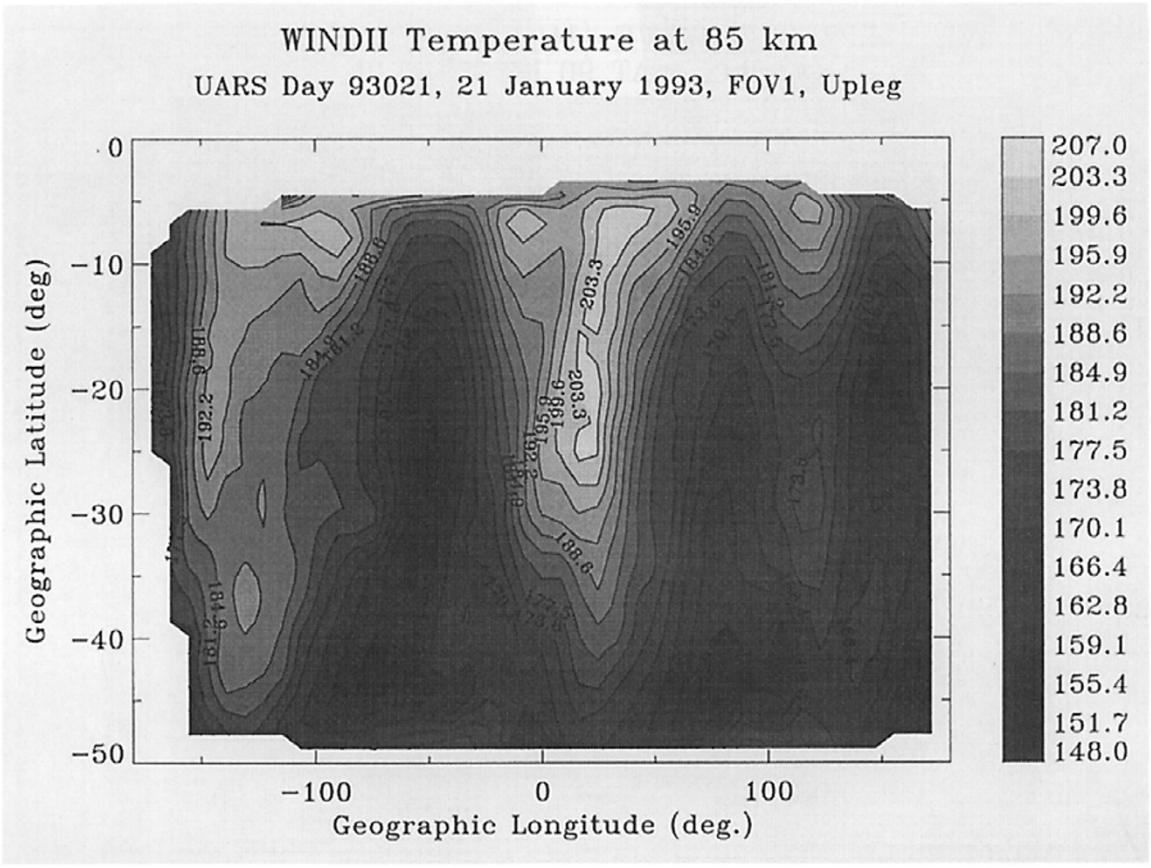

Fig. 1b. Map of the WINDII temperatures at 85 km, in the Southern hemisphere for January 21, 1993. The colour table units are for temperature in Kelvin (K).

The quasi two-day analysis is accomplished employing the approach used for the analysis of WINDII wind data (Ward *et al.*, 1996). The daily longitudinal coverage allows planetary wave signatures to be identified in a single day although in the analysis presented here two day intervals are used to provide better signal-to noise in the determination of the amplitudes and phases. For the tidal analysis the data are binned in local solar time LT/latitude/altitude. The LT binning is 1 hour, the latitude binning is in 10° intervals, and the altitude bins are 2 km. Due to the fact that WINDII views at a fixed angle with respect to the local spacecraft horizontal, the ellipticity of the orbit and the earth oblateness cause the height range of the mesospheric image to change with latitude along the orbit. From the equator to 50°S the height of the bottom of the image changes from 65 km to 80 km restricting the height range available for temperature measurements. Another restriction on the local time coverage is due to the precession of the orbit. For the time period under consideration, the coverage of the northern latitudes is limited by the position of the terminator. Finally, changes in the WINDII observation mode (from Southern to Northern hemisphere), that is the yaw, also lead to a gap in the LT sampling as will be shown and discussed in the following sections.

3. Results

It is well known now that the two dominant planetary scale components in the mesosphere are the migrating solar tides and the westward propagating family of planetary waves. Tidal and planetary waves often dominate the meteorology of the atmospheric region between 80 and 150 km. Thus it is of considerable interest to see to what extent the WINDII temperature observations in the upper mesosphere reflect the presence of such dynamical structures.

3.1 Quasi 2-day wave

Ground-based (Clark *et al.*, 1994; Harris, 1994; Meek *et al.*, 1996) and satellite observations (Wu *et al.*, 1993; Ward *et al.*, 1996) have shown the QTDW to be a dominant dynamical feature in the MLT region in the month following solstice. While most of the results were concerned with the MLT wind field, QTDW signatures were observed also in the mesospheric temperature (Rodgers and Prata, 1981; Wu *et al.*, 1996) and the green line emission rates, observed by WINDII (Ward *et al.*, 1997).

Maps of the temperature field at 85 km were produced for the period of January 19 to January 30, 1993 using individual temperature profiles obtained from the Rayleigh scattering images along the UARS orbit. For the observation period the WINDII instrument was looking southward (viewing range 42°N–72°S) and the orbit was oriented so that the northern hemisphere was in darkness. The period was characterized by a peak amplitude of a QTDW event (Wu *et al.*, 1993, 1995, 1996; Ward *et al.*, 1996). These maps cover a latitudinal range from the equator to about 50°S. As the satellite moves southward the bottom altitude of the WINDII mesospheric image increases so that at latitudes greater than 50°S the bottom altitude is above 85 km and no meaningful Rayleigh

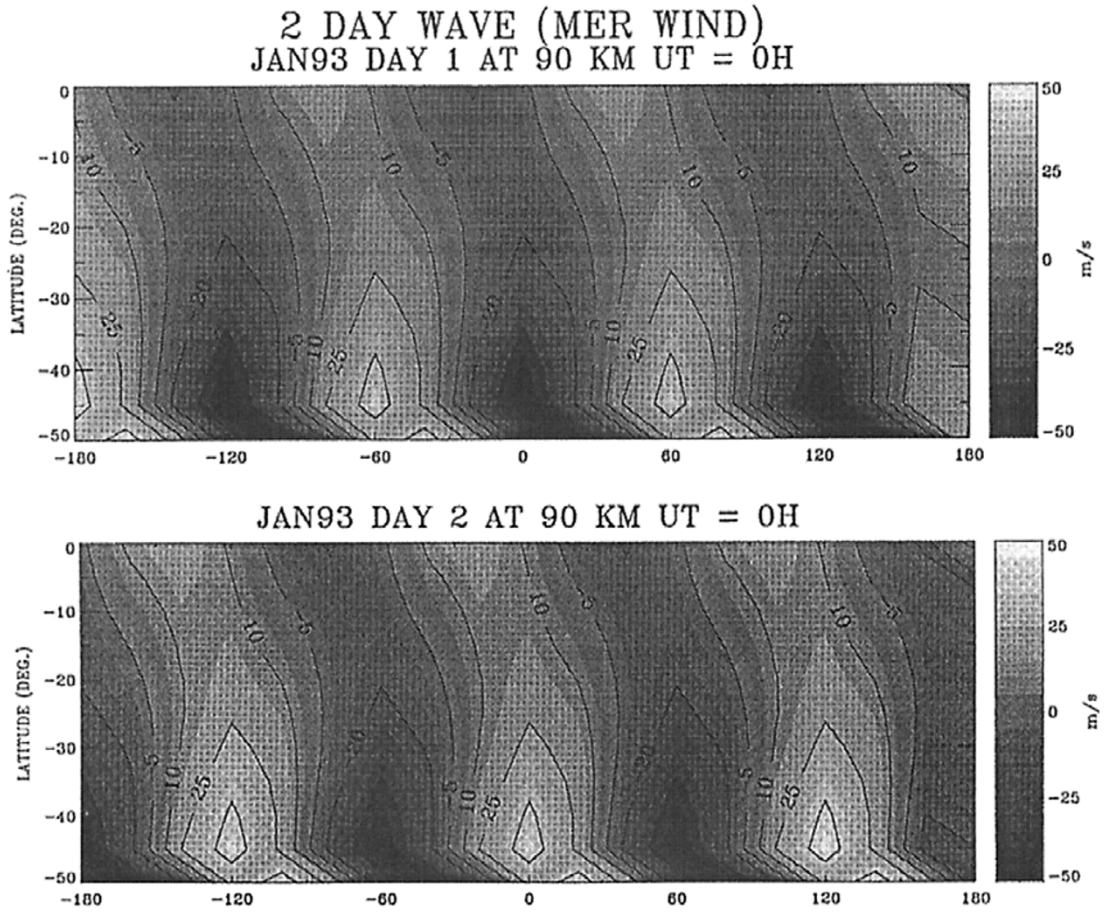

Fig. 2. Simulations of the quasi two-day wave using WINDII wind measurements for January 1993 (see text).

scattering can be observed or temperature derived. In the spring of 1994 this problem was eliminated as the entire UARS satellite was "tipped" downward by about 0.3°.

Mapping of the temperatures at 85 km showed structures in the temperature field characterized by three maxima, each extending from the equator to about 50°S. On a given day these maxima were positioned about 120° longitude apart. Comparing the pattern on two consecutive days, e.g. January 20 and January 21, 1993, illustrated in Fig. 1, showed that on the second day the maxima had propagated westward in longitude with a phase shift of about 60°. All these characteristics are consistent with the signature of a quasi 2-day wave (QTDW) (Hagan *et al.*, 1993). Empirical model fits (Wang *et al.*, 1997) at 90 km height of a QTDW, using high resolution global wind data derived from the WINDII green line observations from 1992 and 1993, and given in Fig. 2, shows a pattern similar with that of the experimental temperatures in Fig. 1.

A comparison between the WINDII meridional wind field on January 20, 1993 at 90 km (Ward *et al.*, 1996, figure 2a) with the temperature field for the same day at 25°–35°S showed winds and temperature QDTW structures to be in quadrature. This is as expected for a Rossby wave with a vertical wavelength significantly greater than two scale heights. The temperature phase fronts are tilted westward similar to the wind QDTW pattern, although the tilt is not very pronounced.

As was mentioned earlier, since the local time at given latitude circle varies by 20 min/day, the 11 day observations encompass about 3.5 hours of local time. Thus as was pointed out by Ward *et al.* (1997) the variations are observed against a background of a mean and a tide at given specific local time.

The amplitude and phase of the dynamical structure seen at 79 km, 82 km, 85 km and 88 km altitude are determined by binning the temperature data into latitude bins of 10°. Each two day period and each latitude bin were fitted in least-mean-square (LMS) sense to:

$$T_{\mathrm{QTDW}} = T_0 + T_{\mathrm{C}} \cos(2\pi(\sigma t + n\phi)) + T_{\mathrm{S}} \sin(2\pi(\sigma t + n\phi)), \tag{1}$$

where: ϕ is the longitude, in degrees, t—the universal time (days), n is the zonal wavenumber (= 3), and σ is the observational frequency (= 0.5 day^{-1}) (Hagan *et al.*, 1993; Wu *et al.*, 1993). Here T_0, T_{C}, and T_{S} are the constants solved for in the fitting process. It is assumed that the central period is 48 hours. The constant T_0, represents the mean temperature and tidal temperature fields (the tidal amplitude being roughly constant during a two-day period), while T_{C} and T_{S} represent components of the QTDW field. The amplitude and phase of the QTDW are given by $\sqrt{T_{\mathrm{C}}^2 + T_{\mathrm{S}}^2}$ and $\tan^{-1}(T_{\mathrm{S}}/T_{\mathrm{C}})$, respectively.

Employing the above expression, the WINDII temperatures were fitted at 20°–30°S and 30°–40°S. Figure 3 illustrates the QTDW fit to the data at 85 km from January 21 and January 22, 1993 at 30°–40°S. The experimental data are indicated with crosses, while the QTDW fit is shown as asterisks. The data are plotted as a function of the fitting phase ($2\pi(\sigma t + n\phi)$) in radians.

The question of aliasing for the QTDW has been discussed by Wu (1994) and Wu *et al.* (1995). The WINDII temperature sampling is such that a data point is obtained for at least one of the legs on both days. According to Wu (1994) the QTDW aliasing is negligible and will not be addressed in the discussion that follows.

From the LMS fit the mean temperature field, amplitude and phase of the QTDW were determined for each day from January 19 to January 30, 1993 and the results at 85 km altitude are given in Fig. 4. The data were fitted separately for upleg and downleg, thus avoiding aliasing due to thermal tidal perturbations. The downleg results are available only for six days, limited by the position of the terminator. The upleg results cover the entire ten days period of observations. A general trend in the temperature amplitudes both for upleg and downleg, as well as at the 20°S–30°S and 30°S–40°S bins, is that they decrease in magnitude as time progresses. The downleg amplitudes show smaller variations but are larger in magnitude than those for the upleg. There seems to be a trend of three-four days of almost constant amplitude, a day of transition, followed by another three to four days of almost constant amplitude particularly at the 30°S–40°S latitude range (Fig. 4b). In the 20°S–30°S range the downleg temperature amplitude is around 16 K for the first three days, followed by another three days with amplitude of about 13 K, giving an average amplitude of 15 K for the entire period. For the upleg the scatter in the 20°S–30°S data is larger but settles down to a mean of about 8 K in the second part of the period (after the 6th day) with an average amplitude of 9 K at 85 km. At 30°S–40°S downleg, the amplitudes

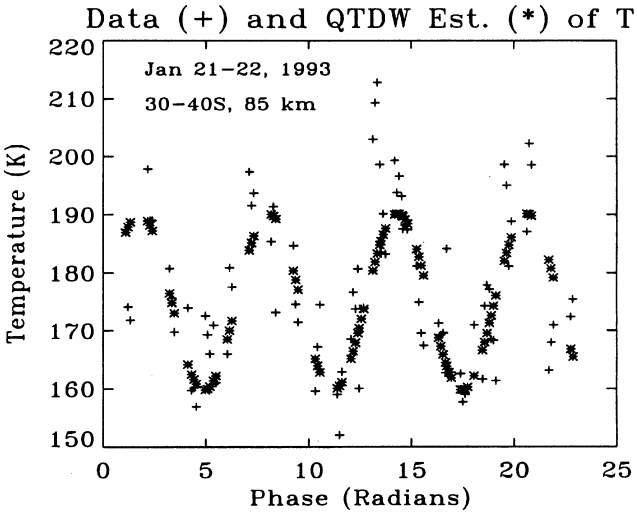

Fig. 3. QTDW fit in LMS sense (asterisks) to the WINDII temperatures (crosses) at 85 km and in the 30°–40°S latitude bin for January 21/22, 1993.

are quite variable ranging from about 16 K for the first three days, to about 9 K at the end of this time interval. For the 30°S–40°S upleg range the amplitude decreases from 14 K in the first four days to about 10 K in the second half of the period, with a total average of 11 K.

The QTDW phase assigned to an arbitrary longitude of 0°, for the downleg is of the order of 12–14 hr for both latitude ranges considered. In the upleg case at 20°S–30°S the QTDW phase varies significantly during the 10 days period with an average of 16 hr, while at 30°S–40°S it is almost constant at about 16 hr. The QTDW mean temperature field including tides, for downleg is of the order of 173–176 K, but larger variations are seen in the upleg data with an average of 176–183 K. In the latitude range 20°S–30°S the QTDW downleg mean temperature at 85 km (Fig. 4a) is rather constant over the six days period, 175–176 K, encompassing 2 hr of LT, while at 30°S–40°S it is of the order of 175 K for the first four days of the period followed by a decrease down to ∼170 K by the end of the time series. For the upleg the scatter of the mean temperatures is larger at the beginning of the observation period, but is about 180 K after the third day at 20°S–30°S, and about 176–177 K at 30°S–40°S.

Figure 5 shows a comparison between the QTDW parameters derived at 79 km, 82 km, 85 km and 88 km for the latitude range 20°S–30°S. In the downleg case the amplitude increases with increasing height from an average of 7 K at 79 km to 15 K at 85 km or by about a factor of 2. In the upleg case the increase is apparent although it is less dramatic and the amplitude of the QTDW at 85 km is only 20% larger than the 79 km value of 8 K. For the 30°S–40°S latitude bin (not shown here) there is much larger scatter both in the downleg and the upleg values compared to those at 20°S–30°S. For the downleg the increase is only 33% larger than the 7 K value at 79 km, while for the upleg—it is about 70% larger than the 6 K value at 79 km.

The differences in the amplitude and mean temperature fields for the upleg and the downleg segments of the WINDII observations seen in Figs. 4 and 5 correspond to different local time and hence to different phases of the tidal signatures or different conditions for the filtering of gravity waves (GW) and the associated forcing of the flow. In a recent study Meyer (1999) investigated the interaction of gravity waves with QTDW employing the GSWM (Hagan *et al.*, 1993) enhanced by a hybrid gravity wave parameterization. The results reported indicate that such an interaction will modify the amplitude of the QTDW while the phase will remain the same. However, the estimated temperature increase of 35 K to baseline QTDW amplitudes of the order of 25–30 K are much larger then the upleg/downleg differences shown in Figs. 4 and 5 and at present we cannot draw a conclusion about the presence or magnitude of plausible GW-QTDW perturbations in the WINDII temperatures.

Wu *et al.* (1996), using temperature data from the UARS/MLS experiment, reported a QTDW temperature amplitude of 7 K at 73 km height (0.046 mb) for late January 1993. An extensive intercomparison between UARS (HRDI and WINDII), ground based radar wind observations and the Global Scale Wave Model (GSWM) (Hagan *et al.*, 1993) predictions for January 1993 performed by Palo *et al.* (1997) has shown that the amplitude of the meridional QTDW at mid-

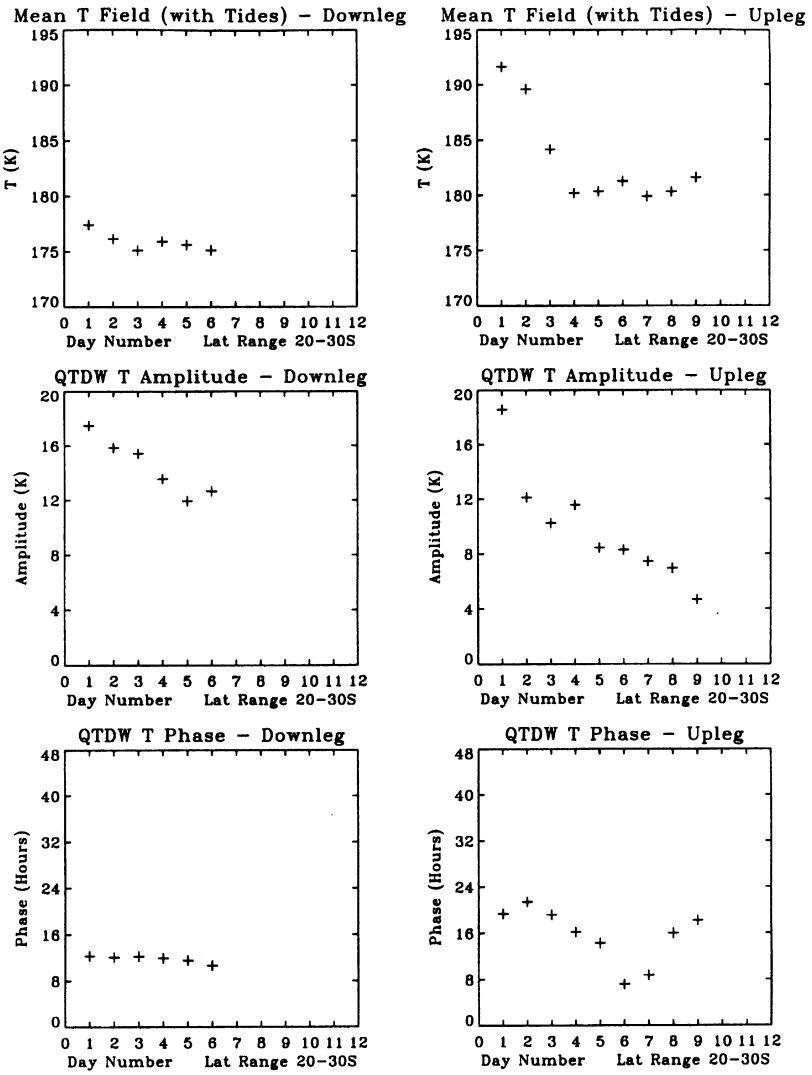

Fig. 4a. QTDW parameters for the WINDII temperature field at 20°–30°S at 85 km altitude.

latitude in the Southern hemisphere increases with height up to about 85 km where the wind amplitude is a factor of 2 larger than that at 75 km (Palo *et al.*, 1997, figure 15). Assuming that there is no significant dynamical perturbation between 73 km and 79 km gives very good agreement between the QTDW temperature amplitudes determined from the MLS and the WINDII observations. The WINDII amplitude results for the downleg are also consistent with the meridional wind QTDW's pattern reported by Palo *et al.* (1997).

3.2 Tidal perturbations

A common approach used in the analysis of dynamical structures in wind data was to combine data from several years of observations for a given season thus producing a larger dataset with better latitude/LT coverage. This approach was demonstrated to be successful in the tidal analysis of the WINDII and HRDI wind data (e.g. Hays *et al.*, 1994; McLandress *et al.*, 1996). While the WINDII wind data have 24 hours coverage allowing reliable determination of diurnal and semidiurnal tidal structures, the WINDII mesospheric temperatures are only for the daytime and the limited LT sampling can influence significantly the characteristics of the results obtained.

Using wind data it has been demonstrated that when a full day of data is averaged to remove the longitudinal variations the pattern is very much in accordance with the classical tidal theory (Hays *et al.*, 1994). In addition to ensuring globally coherent structure zonal averaging also reduces the random instrumental error in the measurements. The WINDII averaging process involves two steps. In the first, for each day the temperatures are zonally averaged over that day enhancing the LT effects, and the second is that a full month of data is binned to cover the full range of local times. As a result different LT come from different days in the month. LT/altitude maps in the height range 72 km–94 km were constructed using the LT/latitude/altitude binned datasets comprising data from the December solstice (24 December–30 January) from 1992/93 and all measurements during the December solstice seasons of 1992/93 and 1993/94. Figure 6 shows the zonal mean temperature field at the equator described by the 1992/93 dataset. At altitudes up to 85 km the maximum temperature contours suggest a downward phase progression with increasing LT in a fashion consistent with a

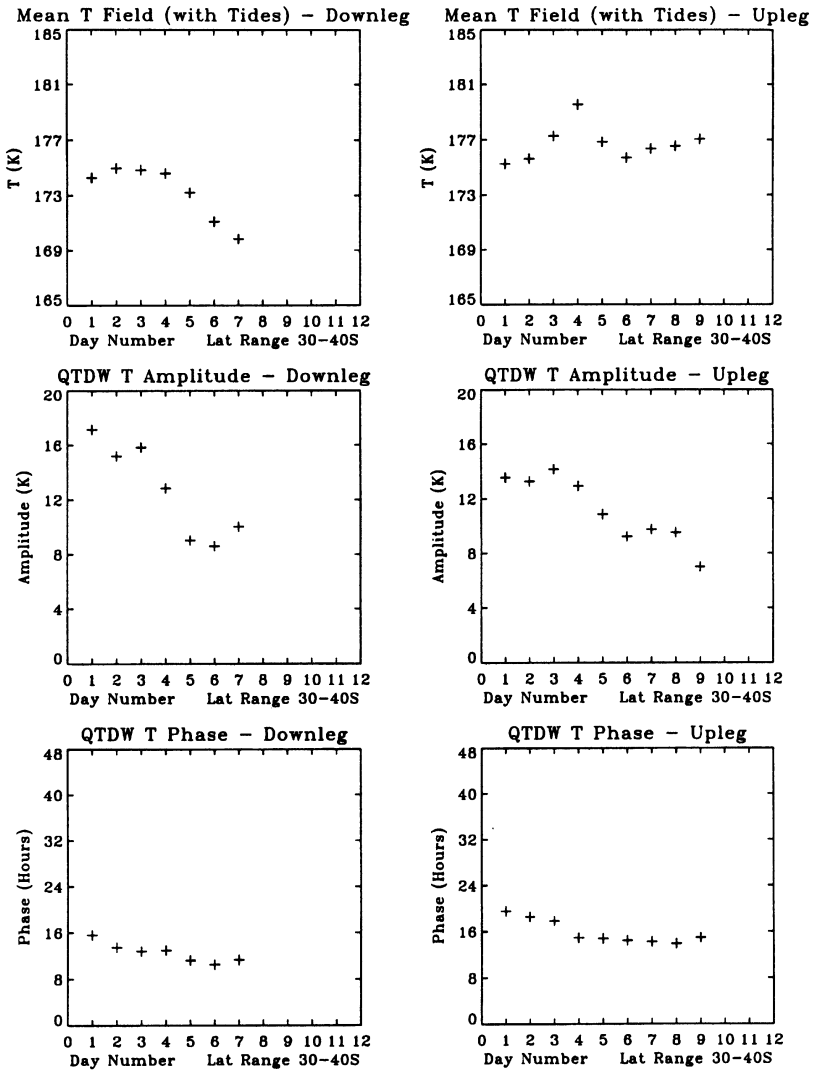

Fig. 4b. QTDW parameters for the WINDII temperature field at 30°–40°S at 85 km altitude.

diurnal perturbation. There is a temperature minimum centered at about 88 km in the morning sector (late January data) which moves slowly upward in the afternoon hours showing a reversed slope to that of the maximum at lower altitudes. This pattern is consistent with observations of tidal temperature perturbations reported by Yu *et al.* (1997). The gap in the LT coverage is due to the yaw change—from one observational mode (Northern hemisphere) to another (Southern hemisphere). Although the yaw requires only one day, the position of the terminator and the WINDII orbital sequence options produce this gap. During the December solstice periods in 1992/93 and 1993/94 the green line emission and the background at 553 nm wavelength are typically observed four times per week during daytime, except for the time from January 19 to January 30, 1993 when measurements were taken every day. In terms of actual time the yaw occurs on January 8, 1993 and January 5, 1994 for the 1992/93 and the 1993/94 datasets, respectively. Combining all temperature profiles for the 1992/1994 period provides more detailed maps of the temperature distribution with height and LT. In the latitude range 15°N–35°S the composite December solstice temperature field is determined from 42 to 45 daily zonal mean profiles. For the 15°N–25°N the sampling is only over 27 days of observations. Figure 7 presents the composite temperature map at the equator—the pattern similar to that outlined by the more limited sampling of the 1992/93 data. There is a distinct downward progression with LT below 85 km height with a well defined mesopause at about 90–92 km height in the morning sector which decreases with height in the afternoon.

A comparison of the 1992/94 zonal mean temperatures in Fig. 7 with TIME-GCM (Roble and Ridley, 1994) predictions of the neutral temperature at the equator for December solstice 1993, given in Fig. 8, shows that the pattern and magnitude displayed in 1992/94 is consistent with the TIME-GCM neutral temperature field for LT from 6 hr to 17 hr and height range from 75 km to 95 km (the range of comparison in Fig. 8 consists of the two unshaded regions, remembering that 12 LT is in the centre of the plot for Fig. 7). In the morning sector there is a minimum in the WINDII zonal mean temperature of 181 K at 7 hr LT and at 88–90 km compared with the 185 K value predicted by the TIME-GCM model at that

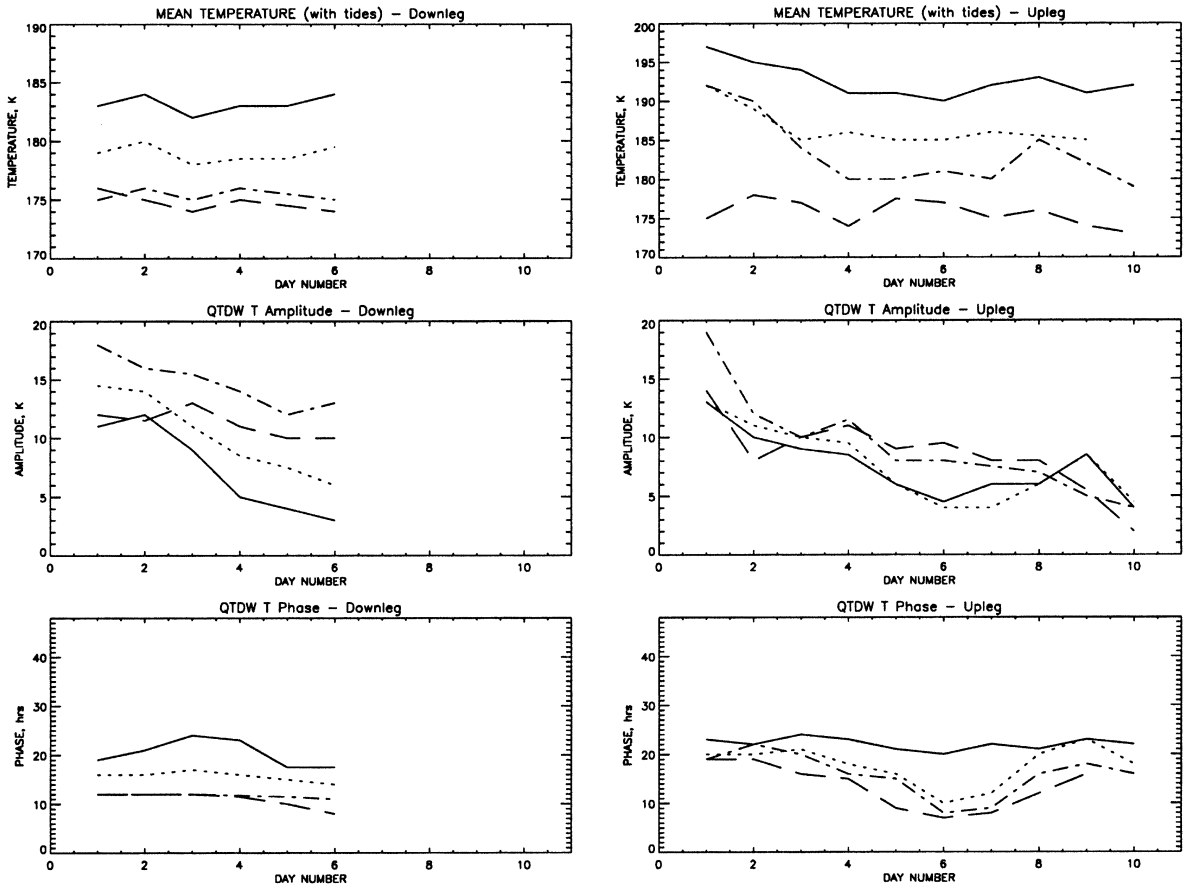

Fig. 5. QTDW parameters for the WINDII temperature field at 20°–30°S for the height range from 79 to 88 km. Solid line—79 km, dotted line—82 km, long-dash—85 km, and dash-dotted—88 km.

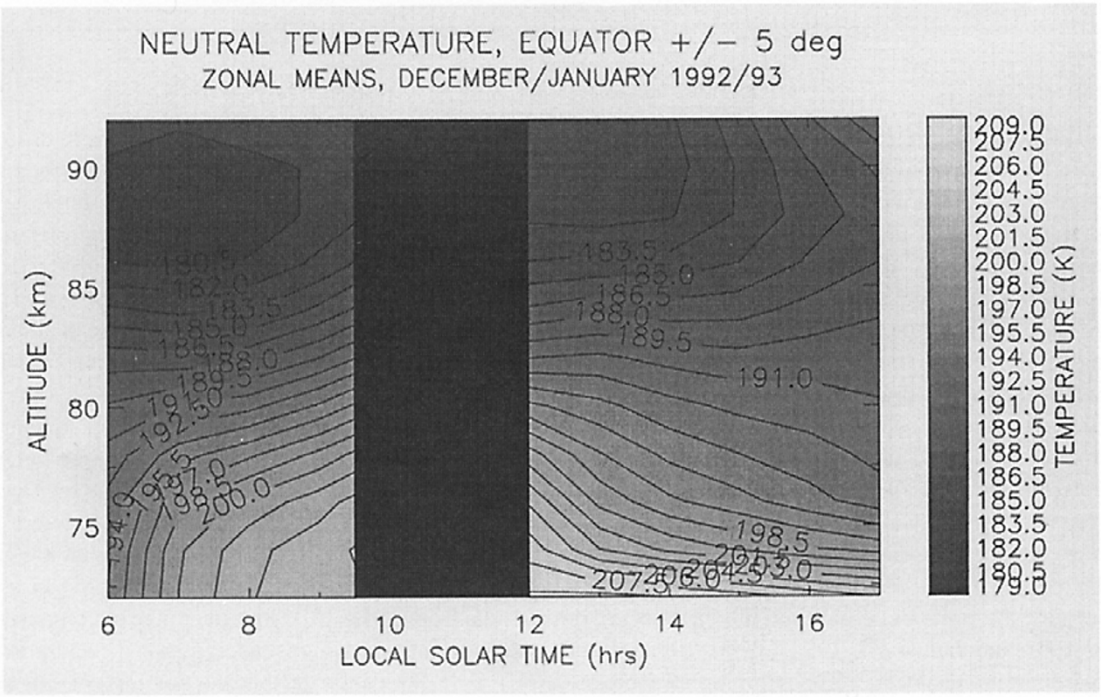

Fig. 6. The WINDII zonal mean temperature field at the Equator, ±5° latitude, for December Solstice 1992/January 1993.

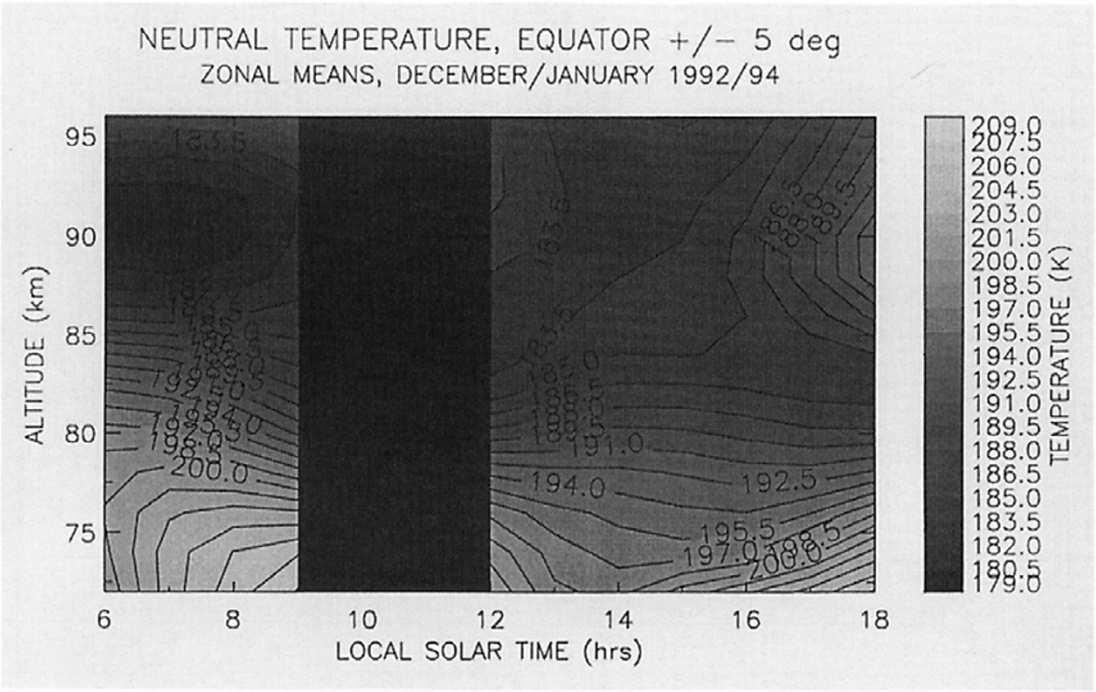

Fig. 7. The WINDII zonal mean temperature field at the Equator, ±5° latitude, for December 1992/93 and January 1993/94.

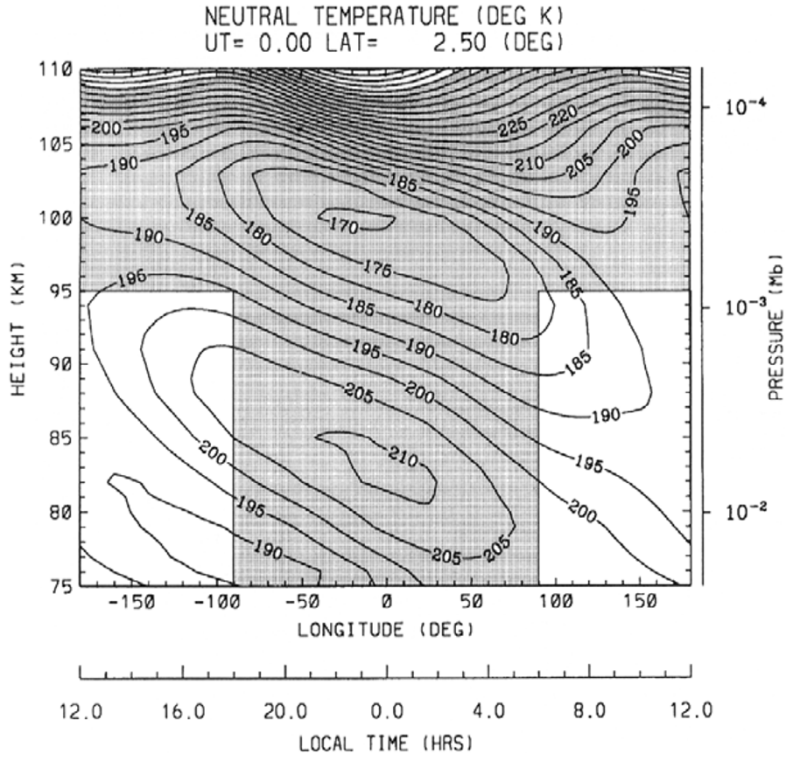

Fig. 8. The TIME-GCM neutral temperature for December solstice at the Equator, 2.5°N. The rectangles outline the LT/altitude range (unshaded) for a comparison with the WINDII diurnal tide amplitudes from Figs. 6 and 7.

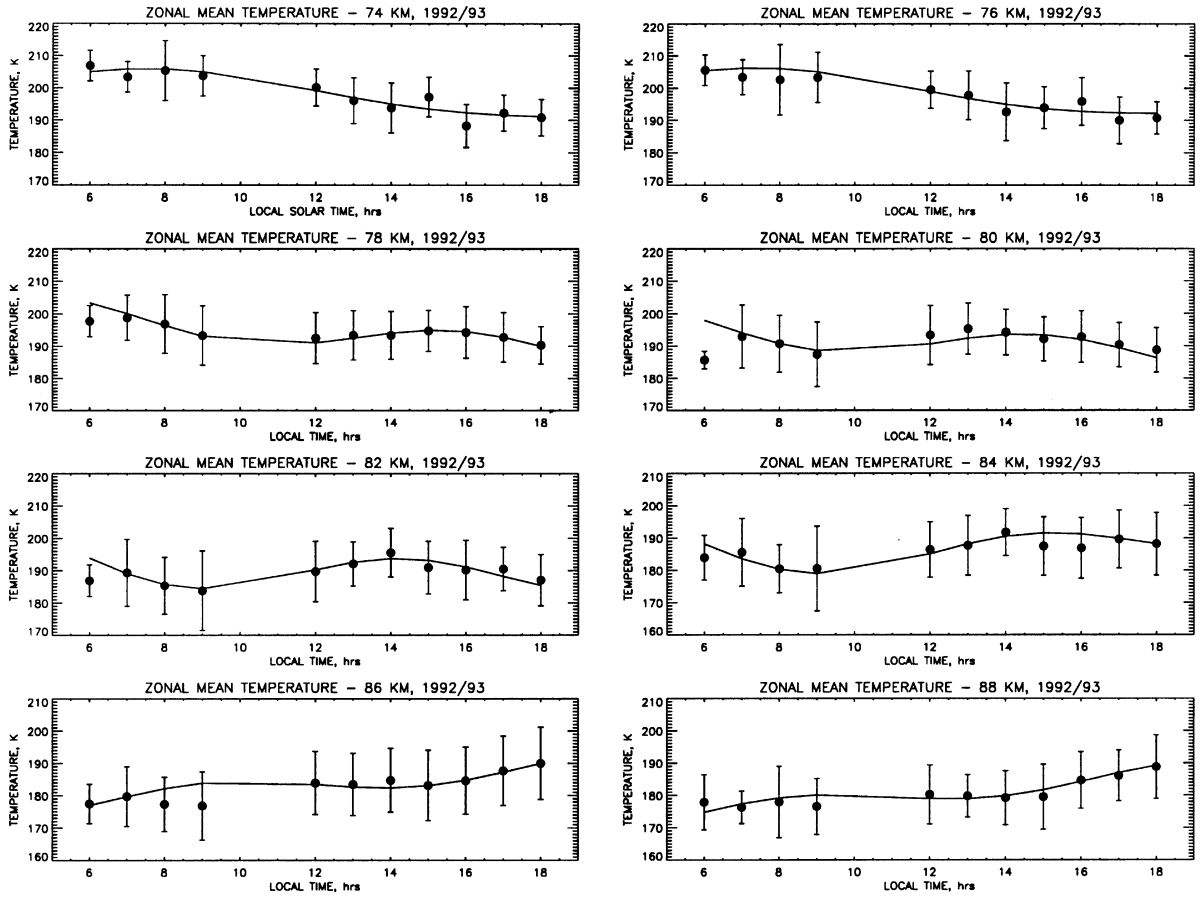

Fig. 9a. LMS fit to the WINDII temperatures at the Equator, ±5°, for December solstice 1992/93. The experimental data are given in solid circles, while the LMS fit is shown with a solid line. The error bars indicate the geophysical variance of the zonal mean daily averaged data.

altitude. The agreement in magnitude in the morning sector remains good at lower altitudes and at 75 km both model and observations give temperatures of about 200 K. In the afternoon sector, the WINDII temperatures are comparable in magnitude with the model below 85 km, but above that altitude the WINDII temperatures are colder by 5–6 K than the TIME-GCM results and show a different pattern from the predicted one. There are local similarities in the pattern of the observed and predicted temperature field, but again in general the descent of the WINDII temperature variations is smaller than the model predictions.

Since the WINDII mesospheric temperatures are restricted to the height range of 72–95 km, a crude estimate of the vertical wavelength of the associated diurnal tidal perturbation is determined as twice the distance between the minimum and the maximum of the temperature field, shown in Figs. 6 and 7. For both, the 1992/93 and the 1992/94 datasets, with minima at about 88 km at 0800 hr LT and maxima at 74 km the vertical wavelength is of the order of 26 km. This value is consistent with the vertical wavelength of 25 km of wind diurnal tides, observed both by HRDI (Hays *et al.*, 1994; Burrage *et al.*, 1995) and WINDII (McLandress *et al.*, 1994). The observed wavelengths are in very good agreement with a vertical wavelength of 26 km for the diurnal temperature tide in the mesosphere predicted by the TIME-GCM, shown in Fig. 8 and also reported by Roble and Shepherd (1997), and Ward *et al.* (1998). We will return to this discussion later in this section.

In general, zonal averaging will remove any contribution of stationary planetary waves to the zonal mean because the averaging is over an integral number of wavelengths. For fast moving travelling planetary waves, such as the QTDW such cancellation will not necessarily occur and aliases might contribute to the zonal averages as has been discussed by McLandress *et al.* (1996) and Forbes *et al.* (1997), and demonstrated by Ward *et al.* (1996) (their figure 1). As was discussed in Subsection 3.1 QTDW have been identified in the late January data corresponding to the morning sector in Figs. 6 and 7. McLandress *et al.* (1996) estimated that the QDTW wave contribution to the daily zonal average was 10% of its amplitude. For amplitudes of the order of 7 K to 14 K (for the height range 79–85 km) the contribution from the QTDW aliasing will be of about 1 K and will be well within the accuracy of the temperature data used to derive the zonal averages.

So far the presence of a diurnal tidal perturbation in the WINDII temperature data has been identified only qualitatively. The traditional method of extracting tidal information from geophysical data is to apply least mean square fit (LMS) to the data. The fit of a diurnal cosinusoidal wave implies that the diurnal signal is dominant in the MLT region at low latitudes.

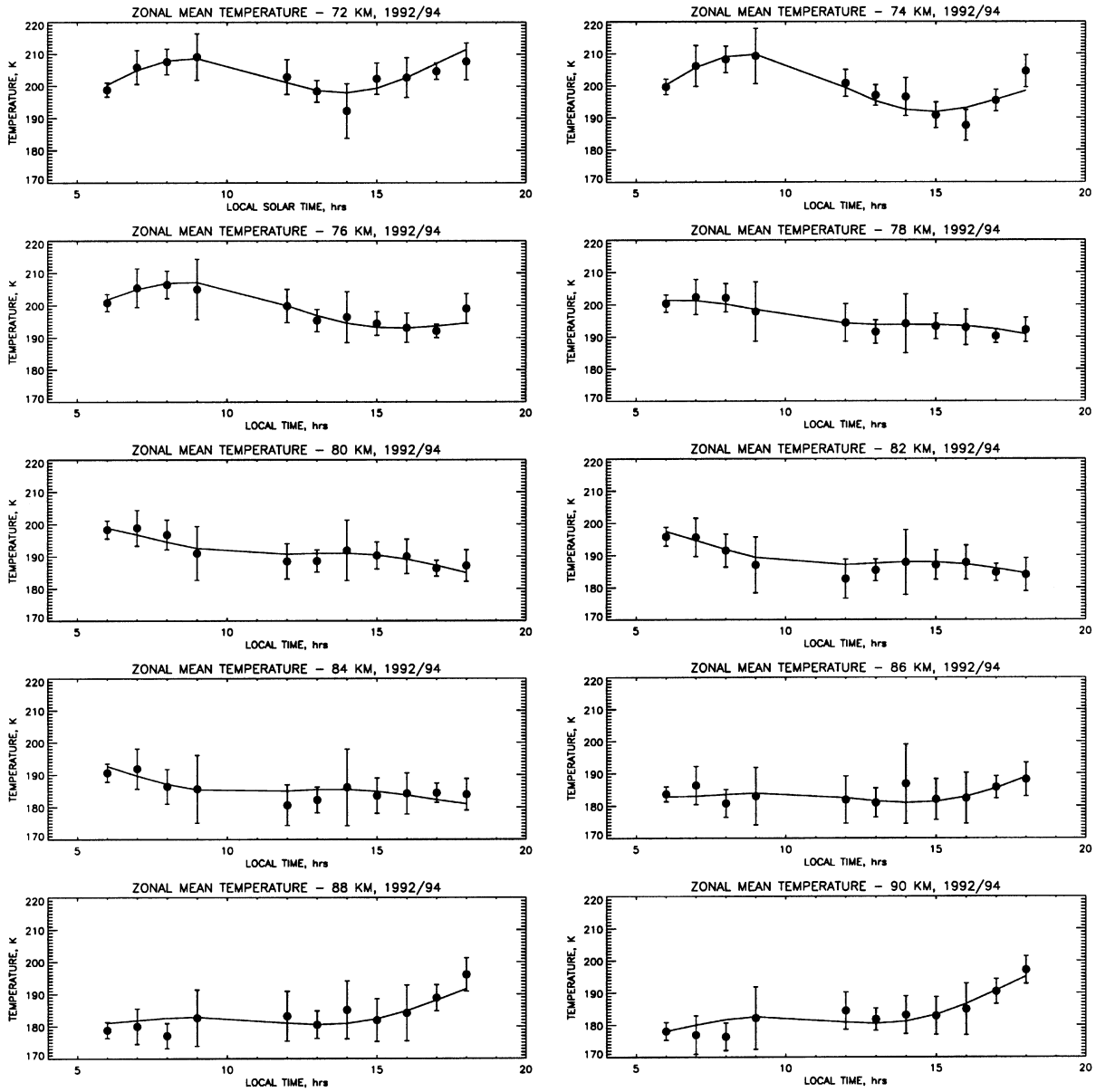

Fig. 9b. The same as in Fig. 9a, but for December solstice 1992/94.

As was mentioned earlier, the temperature data are binned onto LT bins of 1 hr and an LMS fit is done for a given latitude range, each day of observation and each altitude bin to the following equation:

$$T = T_0 + A_{\mathrm{DT}} \cos(2\pi\omega_{\mathrm{DT}}(t - t_0^{\mathrm{DT}})) + B_{\mathrm{ST}} \cos(2\pi\omega_{\mathrm{ST}}(t - t_0^{\mathrm{ST}})), \quad (2)$$

where t is the local time (hr), ω is the frequency ($= 0.042\,\mathrm{hr}^{-1}$ and $0.083\ \mathrm{hr}^{-1}$ for diurnal (DT) and semidiurnal (ST) tide, respectively). The A_{DT}, B_{ST}, t_0^{DT} and t_0^{ST} are the constants solved for in the LMS fitting process giving the amplitude and the phase of the diurnal (DT) and semidiurnal (ST) tide, while T_0 is the mean temperature field. This is "simple binning" (McLandress *et al.*, 1996) since no effort has been made to remove the mean from the tides before sorting the daily zonal averages in local time. As McLandress *et al.* (1996) have shown this method is most suitable for discontinuous data coverage like the data employed in the current analysis.

Since the data are only from daytime observations, with an LT coverage of 9–12 hr between 35°S and 25°N latitude, fitting them directly with the above expression can give ambiguous results. Crary and Forbes (1982) demonstrated that such a time range is insufficient for reliable separation of the diurnal and semidiurnal components and the daily mean. Since the WINDII data are binned in 1 hour bins according to these authors the minimum criterion for reliability of the diurnal tide fit is to have a standard deviation that is less than 3 times the standard deviation of the original data. However, Burrage *et al.* (1995) demonstrated that in spite of the LT limitations of the daytime sampling it is possible to estimate diurnal tidal amplitude and phase, since monthly mean profiles of the diurnal tide are relatively stable in latitude and altitude, being dominated by the tidal mode corresponding to the (1, 1) Hough function. Thus, through various combina-

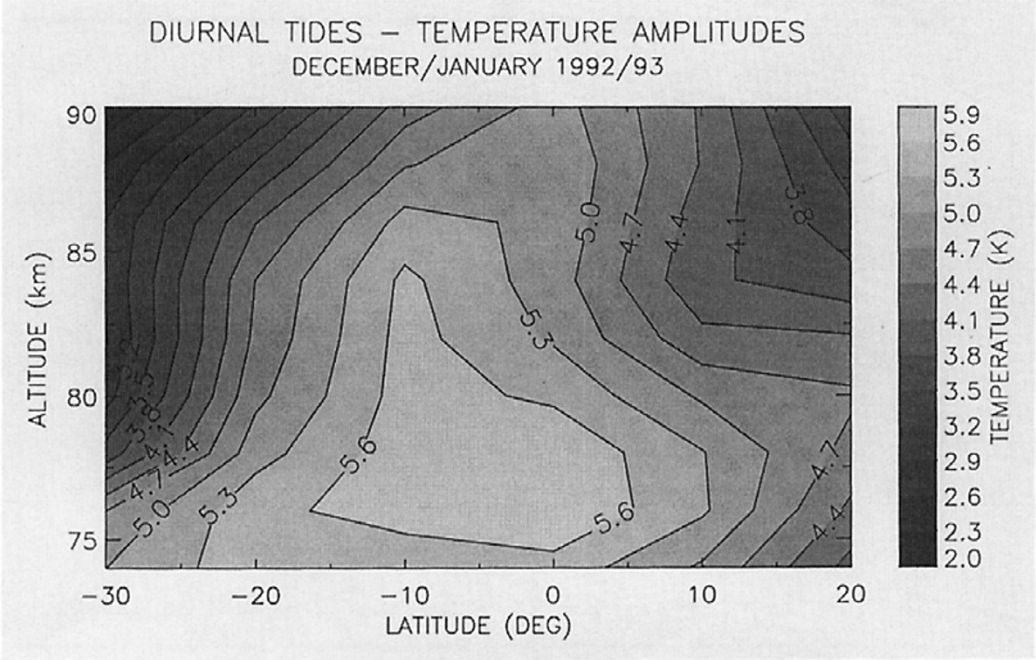

Fig. 10a. The diurnal-tide temperature amplitudes for December 1992/January 1993.

tion trials for the mean temperature and the tidal amplitudes and phases, the best fit to the experimental data was obtained. The results from the LMS fit to the WINDII temperature data at altitudes ranging from 74 to 90 km for a latitude band of ±5° around the equator for December solstice 1992/93 are given in Fig. 9a. The experimental temperatures are given with dots, while the LMS fit for diurnal and semidiurnal tides are given with a solid line. The error bars indicate the geophysical variance (the standard deviation) of the zonally averaged daily mean temperatures for given latitude bin and a LT range from 6 hr to 18 hr. Although a significant amount of variation was observed from orbit to orbit which may be caused by longitudinally varying planetary-scale disturbance (Shepherd *et al.*, 1993b) more often than not a distinct similarity in the shape of the temperature profiles was observed (not shown here for brevity), in particular for the 15°N to 25°S latitudinal bins. This underlying structure is suggestive of the presence of the migrating solar tides and the background mean temperature field and is in concert with the pattern shown in Figs. 6 and 7. Although in general the LMS fit to the daily zonal mean temperatures is rather good, one should bear in mind that at altitudes above about 90 km the quality of the WINDII data decreases in relation to the decrease of the SNR and the determined amplitudes and phases could be erroneous. Therefore although there are temperature data up to 95 km we have chosen to discuss results only below 90 km altitude. Figure 9b presents the results of the LMS fitting of the 1992/1994 combined datasets at the equator along with the standard deviations of the experimental data for the altitude range from 72 km to 90 km. In view of the above discussion the tidal parameters obtained in the analysis will be compared with other independent results to establish their acceptability.

Due to the WINDII viewing geometry and the position of the terminator the number of LT samples at latitudes greater than 25°N was not sufficient to extract meaningful information on either the diurnal or semidiurnal tides and so data above this latitude are not shown or discussed herein. Figure 10 gives the latitudinal pattern of the diurnal tidal amplitudes obtained according to the WINDII observations at altitudes from 74 km to 90 km, for December solstice 1992/93 and for the composite 1992/94 data in the height range 72 km to 90 km. The (1, 1) diurnal-tide amplitude of the temperature has a maximum at the equator with a value of 5–6 K, decreasing towards subtropical latitudes (±20°). Such pattern in the experimental data is consistent with the Hough function for the diurnal temperature tide. In addition, the contours suggest a tilt southward, increasing with height to about 83–85 km, which then reverses to northward at higher latitudes. The tidal amplitude is somewhat asymmetric about the equator. As in the case of wind diurnal tides (Hays *et al.*, 1994, McLandress *et al.*, 1996) this may be due to changes in the mean winds and temperature gradients giving rise to higher-order modes other than the classical (1, 1) diurnal tide. An indication of such changes will be seen in the corresponding phases shown in Fig. 11. As was discussed earlier, McLandress *et al.* (1996) and Forbes *et al.* (1997) suggested that the correct determination of the tidal amplitude could be affected by the presence of a QTDW perturbation if the tidal amplitude is less than 10% that of the QTDW. Comparing the tidal and QTDW temperature amplitudes obtained in the analysis shows that the tidal amplitude is 50% of the QTDW amplitude and thus is not distorted significantly by the QTDW perturbation.

The diurnal-tide amplitudes of the composite 1992/1994 data as shown in Fig. 10b, for the latitude range 20°N–20°S. At latitudes ±15° around the equator the amplitudes are of the same magnitude of 5–6 K as those in 1992/93 but the distribution around the equator is more symmetrical than that for the 1992/93 season. There is a locus at ∼20°N latitude

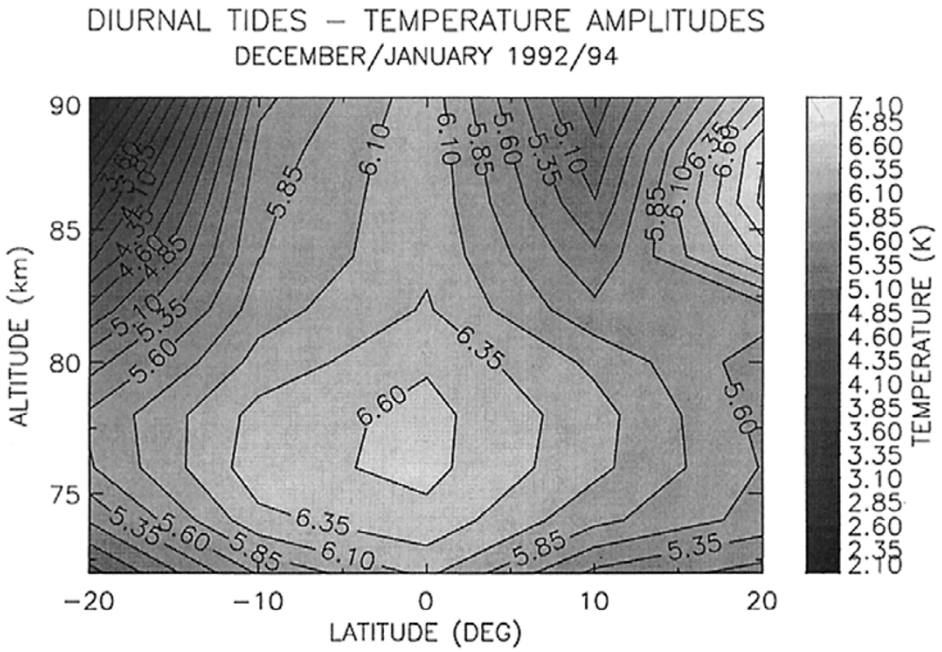

Fig. 10b. The diurnal-tide temperature amplitudes for December 1992/93 and January 1993/94.

appearing at altitudes above 85 km and an amplitude comparable to that at the equator. The general pattern is similar to the composite daily zonal mean neutral temperatures given in Fig. 7, for the 16–18 hr LT range. The temperatures in this LT range are from December 24–31 period and are mostly from the 1993/94 dataset.

Differences between the tidal structures in the 1992–93 and 1993–94 wind data were observed and discussed by Burrage *et al.* (1995) and Yudin *et al.* (1997). Applying root-mean-square (rms) wind analysis Yudin *et al.* (1997) found that the 1992–93 monthly mean composites have similar patterns and locations of the tidal-wind energy concentration. The 1993–94 wind rms showed a much weaker concentration of kinetic energy in the lower latitudinal MLT region. Such attenuation of the (1, 1)-mode diurnal amplitudes after September 1993 have been previously reported by Burrage *et al.* (1995). More recent analysis by Zhang *et al.* (1998) of the tidal structure variation of O(^{1}S) volume emission rates observed by the WINDII over the period 1992–1996 have also shown a decrease in the tidal amplitude at low latitudes over these years. Although those observations are not linearly related to the neutral temperature in the middle atmosphere/lower thermosphere (MLT) region it is reasonable to assume that the temperature structure should also experience variations consistent to those observed in the wind and emission rate field.

Figure 11a shows the phase (LT of amplitude maximum) for the diurnal tide obtained from the LMS fit to the 1992/93 temperatures. The phases are presented for 10° bins from 35°S to 25°N. At all latitudes considered the diurnal tide exhibits a systematic downward phase progression with latitude. It has been suggested (Hays *et al.*, 1994) that latitudinal changes in the phase indicate the presence of more than one Hough mode. At the equator (±5°) the diurnal phase has a well defined period of 24 hours and an inferred vertical wavelength of about 24 km. However, away from the equator (latitudes greater than ±5°) the slopes of the respective phase profiles are more consistent with a semidiurnal tide with a period of 6–12 hr and a vertical wavelength of more than 41–43 km. The transition seems to occur at the 5°–15° latitude band along the equator and at about 85 km height. At altitudes below 85 km tidal structures with a wavelength of ∼32 km suggest a semidiurnal component to the tidal perturbation, while above 85 km the diurnal tide component is still present at higher latitudes (>15°–25°S). We now turn to the diurnal temperature phases for the 1992/94 data, shown in Fig. 11b. At the equator (±5°) and at latitudes up to about 10°S (5°S–15°S latitude bin) the inferred vertical wavelength is 24–26 km and the phase range is ∼24 hr or that of a diurnal tide. In the last bins for each hemisphere the pattern is similar to that observed in the 1992/93 data, namely that slope changes with a divide at about 85 km. North of the equator the inferred vertical wavelength for latitudes below 90 km is ∼38–40 km with a phase range of only 10 hr and suggests the presence of a semidiurnal-type tide rather than a diurnal one. At altitudes above 90 km the temperature data become increasingly noisy and should be viewed with caution. In the South at 15°S–25°S and 25°S–35°S the presence of other tidal modes becomes rather obvious both in the change of phase at ∼85 km and in the slope of the phase below that altitude. The inferred vertical wavelength is 36–46 km. At both latitudes the sampling is over 12 hr and 11 hr of LT, respectively. The results shown in Fig. 11 suggest that for December solstice conditions meaningful diurnal (1, 1) tide information can be extracted only for latitudes of ±10°–15° around the equator. At higher latitudes the inferred vertical wavelengths are consistent with the (2, 5) and (2, 6) modes of the semidiurnal tide (i.e. Forbes, 1995). As the sampling

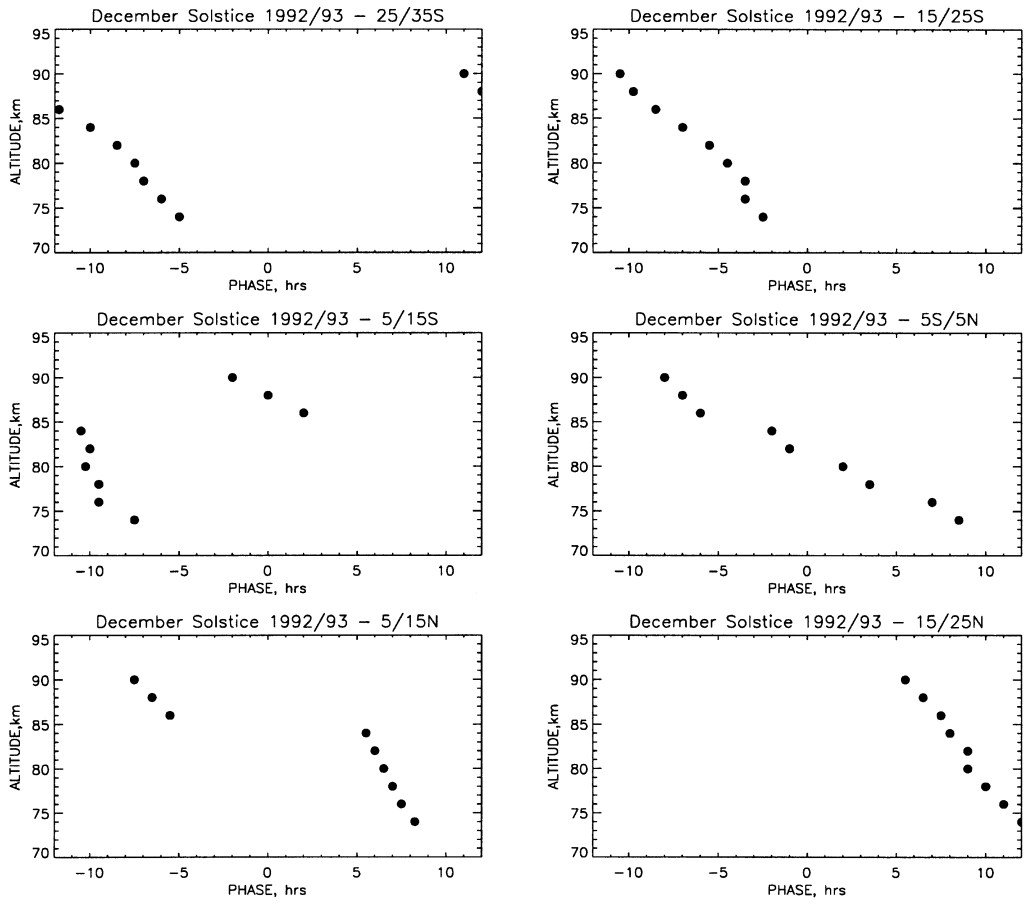

Fig. 11a. The diurnal-tide phases of the WINDII temperatures for December 1992/January 1993.

in LT decreases (as in the case at 15°N–25°N) or the difference between the ascending and descending part of the orbits is less than 12 hr the uncertainty in the derived tidal parameters increases significantly in agreement with the results presented by Crary and Forbes (1982).

Burrage *et al.* (1995) studied seasonal variations of wind semidiurnal tides and found that they are stronger at solstice than at equinox, opposite to the diurnal tides which maximize at equinox and are much smaller at solstice. Shepherd *et al.* (1998) reached the same conclusion from the analysis of the WINDII meridional winds. Our analysis shows that the semidiurnal tidal amplitudes are larger in magnitude that the diurnal ones with a maximum at about 20°S. At the equator the amplitudes are comparable (∼5–6 K). However, it has been pointed out (Hays *et al.*, 1994; Burrage *et al.*, 1995) that LMS fitting of daytime wind data cannot provide reliable estimate of the semidiurnal tidal parameters and this discussion of our semidiurnal results is outside the scope of this report.

According to Ward (1998), the temperature oscillations at a given height are dependent on the form of the background temperature profile at that height. Thus comparisons of temperature amplitudes between different datasets and between models and experimental data must take account of differences in the background temperature profiles for appropriate comparisons to be conducted.

Since mean temperature fields using the same dataset were determined independently both in the QTDW and the tidal analysis, as a check for consistency it is important to compare the magnitude of these results. At 79 km the mean temperature from the tidal analysis (Fig. 12) is 185 K at 25°S while from the QTDW analysis (Fig. 5) it is 187 K and 195 K for the downleg and upleg, respectively. Since the mean temperature for the tides is determined from both upleg and downleg data the average mean temperature for the QTDW is 191 K, including tides. The difference of 6 K is of the order of the tidal amplitudes at 79 km as can be seen in Fig. 10. At 85 km the mean temperature from the tides is 182 K compared to the average QTDW mean of 180 K, and thus giving a difference of 2 K between the two analytically determined mean temperature fields at that altitude. Although it is expected that the QTDW's mean and tidal temperature field should be larger than the mean temperature from the tidal analysis, the relationship at 85 km is reversed. A possible reason may be due to the fact that the latitudinal sampling of the QTDW is slightly different from that in the tidal analysis, that is at 20°S–30°S and 30°S–40°S for the QTDW compared to the 15°S–25°S and 25°S–35°S for the tides. Thus temperature profiles contributing to the lower latitude end of the tidal 15°S–25°S range and having higher zonal averages, are not included in the QTDW 20°S–30°S sampling, while at the upper end of the QDTW range colder temperatures from higher latitudes (from 25°S–30°S in the 20°S–30°S range and from 35°S–40°S in the 30°S–40°S range) contribute to the results

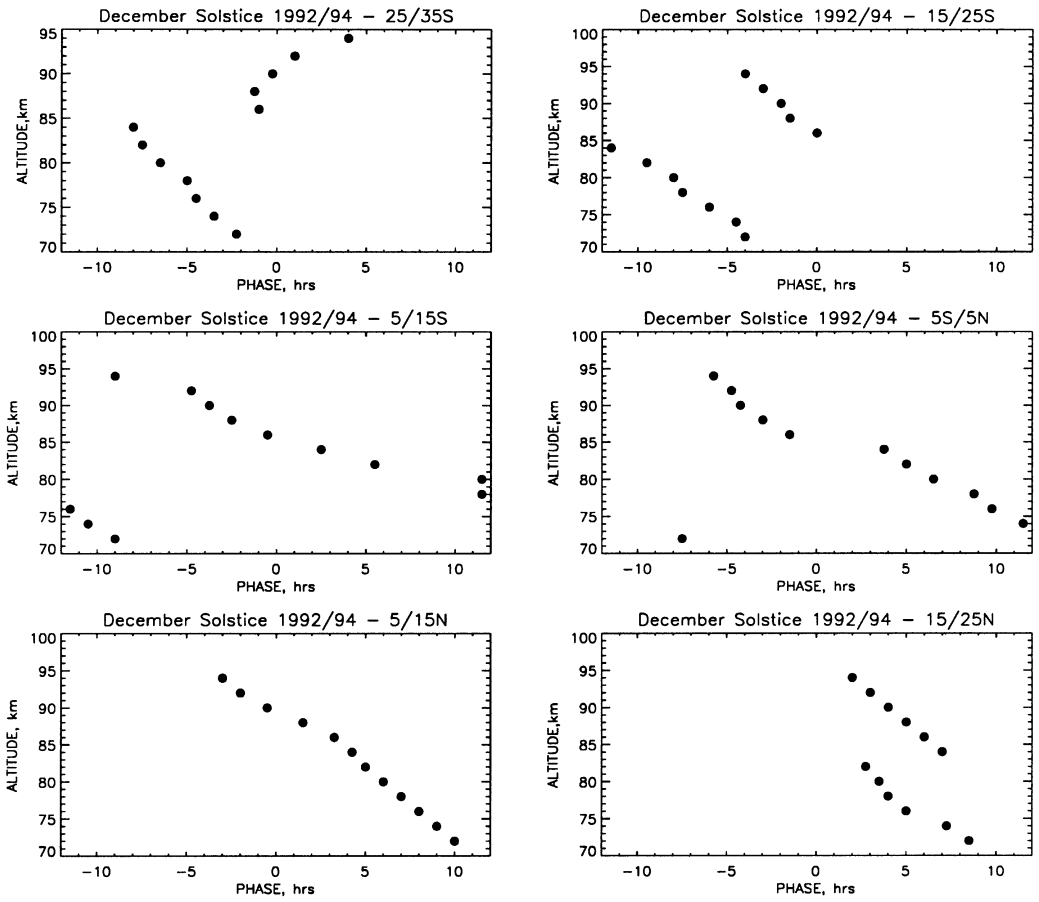

Fig. 11b. The same as in Fig. 11a, but for December 1992/93 and January 1993/94.

obtained. With all this in mind we consider the LMS results for the mean temperature QTDW and tidal fields to be in acceptable agreement.

To test further the results from the LMS fit to the WINDII temperatures, the WINDII diurnal amplitudes given in Fig. 10a are compared with predictions for December solstice for January 1993 from the TIME-GCM model, shown in Fig. 13 as an unshaded rectangle. There is an agreement in the magnitude of the diurnal-tide amplitude, from the 1992/93 season and the TIME-GCM predictions within the latitude/height range of the observations. A tilt in the maximum/minimum pattern towards the South hemisphere is seen both in the WINDII data and the TIME-GCM predictions. However, more detailed analysis is necessary for better quantitative comparison between the WINDII results and the model predictions.

4. Discussion

The analysis presented showed that in spite of the limited local time coverage of the WINDII mesospheric temperatures (only 10–12 hr) the LMS fit applied to data in the $\pm 15^\circ$ latitude range around the equator can provide a realistic estimate of the diurnal tidal amplitudes and phases of the mesospheric temperature in the height range 72–90 km that is consistent with the classical tidal theory. The magnitude of the WINDII diurnal amplitudes is comparable with the TIME-GCM model, but the pattern differs for latitudes greater than 10°–15° around the equator. Since the TIME-GCM model has been shown to agree with the WINDII O(^{1}S) airglow and wind observations with a full 24 hr LT coverage (Roble and Shepherd, 1997; Shepherd *et al.*, 1998) and since the WINDII temperatures are derived from the Rayleigh scattering measurements from the O(^{1}S) background filter, we consider the reasonable agreement in the $\pm 15^\circ$ latitude range to be in support of the potential consistency between the WINDII mesospheric temperatures and meridional winds at those latitudes.

All temperature tidal results presented here are for December solstice conditions, when the diurnal tidal amplitudes are very weak and can be affected by other Hough modes as was illustrated by the derived diurnal phases. A further test of the method and results presented so far will be an analysis and comparison of the WINDII mesospheric temperatures with model predictions and other experimental data for spring equinox, which is currently under way.

5. Conclusions

We have presented observations of the mean temperature, quasi-two-day wave and diurnal tides from the upper mesosphere for December solstice, during December 1992/1993 and January 1993/1994, observed by WINDII.

Although the database did not provide a full LT coverage for complete tidal analysis it was demonstrated that the WINDII daytime temperature dataset allows the determina-

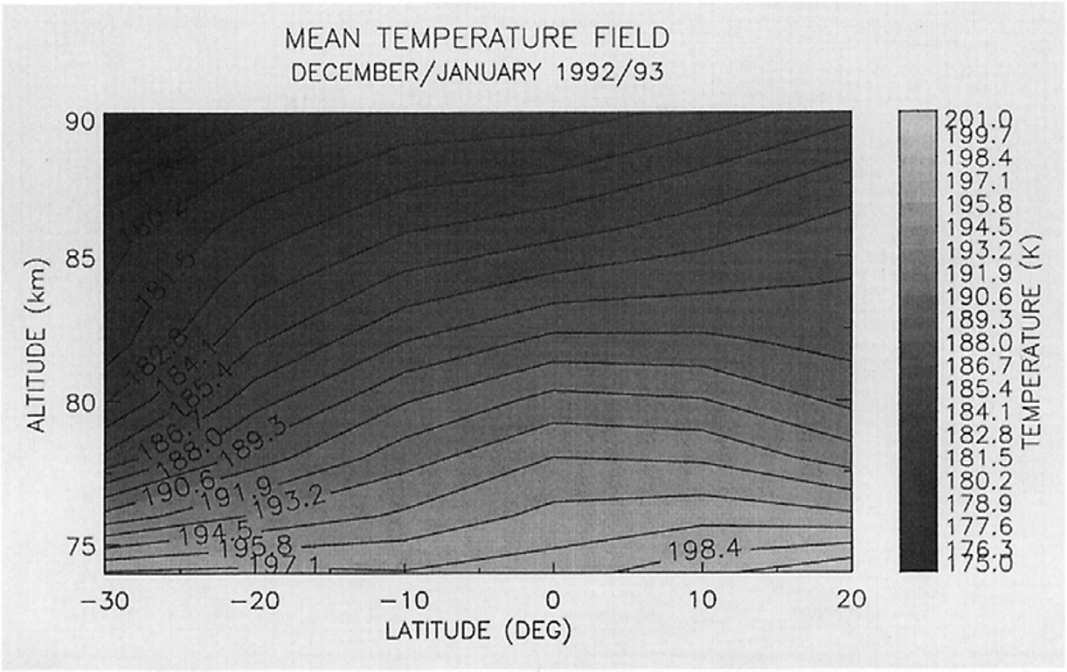

Fig. 12a. WINDII mean temperature field for December 1992/January 1993—a LMS fit to the WINDII temperatures.

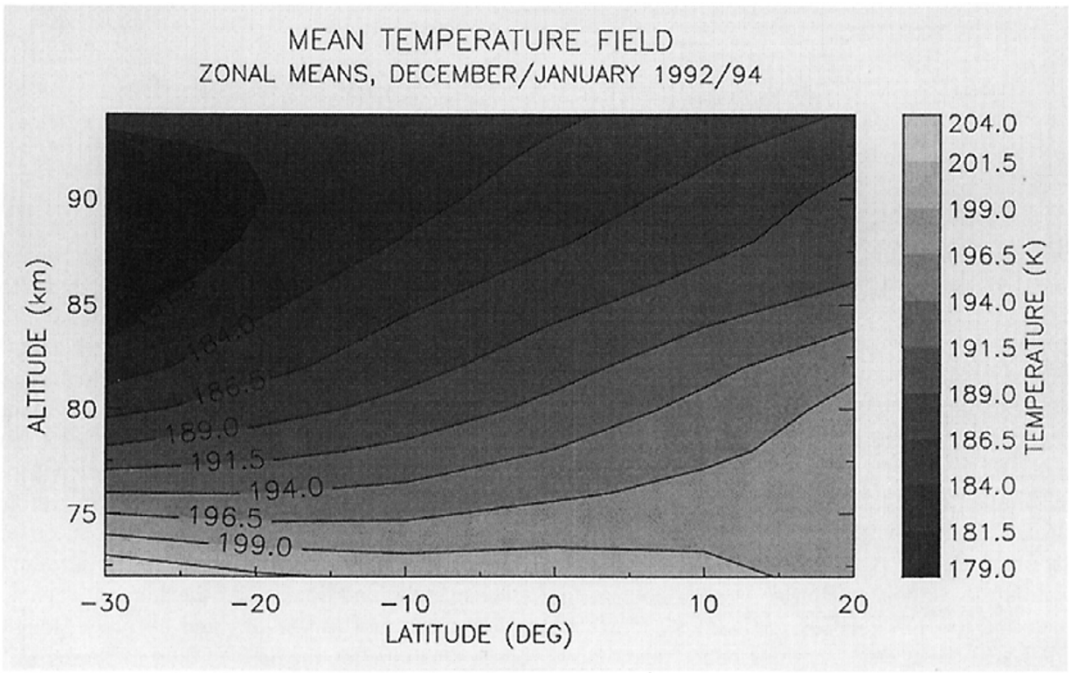

Fig. 12b. WINDII mean temperature field for December 1992/93 and January 1993/94—a LMS fit to the WINDII temperatures.

tion of planetary wave and tidal structures, which characteristics are in good agreement with other independent temperature observations and model simulations.

The main results of the work presented are as follows:

1. The planetary wave structures observed are well described with a quasi two-day wave, $n = 3$. The amplitude, for a latitude range between 20°S and 40°S at 85 km where the wave amplitude maximizes, is about 15 K for downleg and 11 K for upleg sampling. It was shown that the WINDII QTDW amplitudes were in good agreement with QTDW temperature results from the MLS experiment on UARS and the vertical amplitude structure of the QTDW, described by the HRDI wind observations.

2. The temperature variability of the QDTW provides a view of the spatial characteristics of the amplitude and phase of this planetary wave structure which were not published before.

3. The mesospheric temperature field described by the

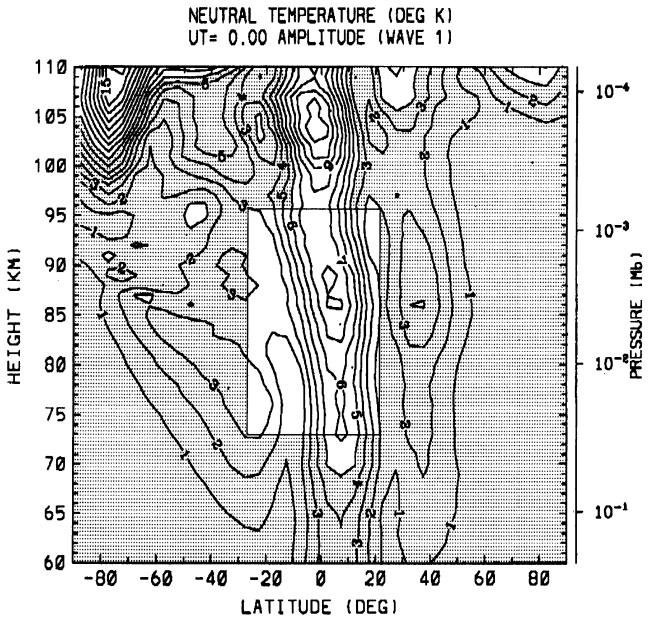

Fig. 13. TIME-GCM diurnal-tide temperature amplitudes for December solstice. The rectangle outlines the latitude/altitude range (unshaded) for a comparison with the WINDII diurnal tide amplitudes from Fig. 10a.

WINDII zonal means for the December solstice periods in 1992/93 and 1992/94, examples of which were presented for the equator, is in agreement in magnitude (within 4–6 K in the height range 75–95 km), with the predictions of the TIME-GCM model, although the overall pattern differs somewhat. However, the WINDII data are highly suggestive of a diurnal variation in the temperature on the same order as predicted by the model. The descent of temperature variations with time seen in the model is not clearly evident in the WINDII results.

4. The tidal pattern in the 70–95 km height range is consistent with that of the diurnal tide with a vertical wavelength of 20 km for the 1992/93 dataset and of 25 km for the 1992/94 dataset at the equator, $\pm 5^\circ$, and at $\pm 10^\circ$ around the equator.

5. At latitudes greater than 15° the tidal phase indicated perturbation of semidiurnal type (period of 6–12 hr) and inferred vertical wavelength greater than $\sim$40 km.

6. For the 1992/93 data the diurnal-tide amplitudes determined for latitudes from 35°S to 25°N maximize at the equator with a magnitude of $\sim$6 K (the actual diurnal amplitudes from the LMS fit at the equator are of the order of 7 K before creating the contour plot) and decrease toward tropical latitudes, consistent with the classical tidal theory and the Hough function for temperature.

7. The mean temperature field for December solstice 1992/93, determined independently both in the tidal and the QTDW analysis, are consistent with each other when compared at 25°S in the height range 79 to 88 km.

Acknowledgments. The WINDII project is jointly sponsored by the Canadian Space Agency and the Centre National d'Etudes Spatiales, France. The authors are grateful for their support, along with NASA, in making this work possible. Support for scientific analysis of the data is provided by the Natural Science and Engineering Research Council of Canada. The Centre for Research in Earth and Space Technology (CRESTech) is a designated Centre of Excellence supported by the Technology Fund of the Province of Ontario. The authors thank Dr. B. H. Solheim for providing the WINDII raw data used in this study. We would also like to thank the referees for their helpful suggestions in the revision of this manuscript.

References

Akmaev, R. A., V. A. Yudin, and D. A. Ortland, SMLTM simulations of the diurnal tide: comparison with UARS observations, *Ann. Geophysicae*, **15**, 1187–1197, 1997.

Burrage, M. D., M. E. Hagan, W. R. Skinner, D. L. Wu, and P. B. Hays, Long-term variability in the solar diurnal tide observed by HRDI and simulated by GSWM, *Geophys. Res. Lett.*, **22**, 2641–2644, 1995.

Chahine, M., Generalization of the relaxation Method for the Inverse Solution of Nonlinear and Linear Transfer Equations, in *Inversion Methods in Atmospheric Remote Sounding*, edited by A. Deepak, Academic Press, pp. 67–116, 1977.

Clancy, R. T. and D. W. Rusch, Climatology and trends of mesospheric (58–90 km) temperatures based upon 1982–1986 SME limb scattering profiles, *J. Geophys. Res.*, **94**, 3377–3393, 1989.

Clancy, R. T., D. W. Rusch, and M. T. Callan, Temperature minima in the average thermal structure of the middle mesosphere (70–80 km) from analysis of 40- to 92-km SME global temperature profiles, *J. Geophys. Res.*, **99**, 19,001–19,020, 1994.

Clark, R. R., A. C. Current, A. H. Manson, C. E. Meek, S. K. Avery, S. E. Palo, and T. Aso, Hemispheric properties of the two-day wave from mesosphere-lower-thermosphere radar observations, *J. Atmos. Terr. Phys.*, **56**, 1276–1288, 1994.

Crary, D. J. and J. M. Forbes, On the extraction of tidal information from measurements covering a fraction of a day, *Geophys. Res. Lett.*, **10**, 580–582, 1982.

Dudhia, A., S. E. Smith, A. R. Wood, and F. W. Taylor, Diurnal and semidiurnal temperature variability of the middle atmosphere, as observed by ISAMS, *Geophys. Res. Lett.*, **20**, 1251–1254, 1993.

Forbes, J. M., Atmospheric tides 1. Model description and results of the solar diurnal component, *J. Geophys. Res.*, **87**, 5222–5240, 1982.

Forbes J. M., Tidal and planetary waves, in *The Upper Mesosphere and lower thermopshere: A review of experiment and theory, Geophysical Monograph 87*, edited by R. M. Johnson and T. L. Killeen, pp. 67–87, AGU, Washington D.C., 1995.

Forbes, J. M., M. Kilpatrick, D. Fritts, A. H. Manson, and R. A. Vincent, Zonal mean and tidal dynamics from space: an empirical examination of aliasing and sampling issues, *Ann. Geophysicae*, **15**, 1158–1164, 1997.

Hagan, M. E., J. M. Forbes, and F. Vial, Numerical investigations of the propagation of the quasi-two-day wave into the lower thermosphere, *J. Geophys. Res.*, **98**, 23,193–23,205, 1993.

Hagan, M. E., J. M. Forbes, and F. Vial, On modeling migrating solar tides, *Geophys. Res. Lett.*, **22**, 893–896, 1995.

Hagan, M. E., C. McLandress, and J. M. Forbes, Diurnal tidal variability in the upper mesosphere and the lower thermosphere, *Ann. Geophysicae*, **15**, 1176–1186, 1997.

Harris, T. J., A long-term study of the quasi-two-day wave in the middle atmosphere, *J. Atmos. Terr. Phys.*, **56**, 569–579, 1994.

Hays, P. B., D. L. Wu, and the HRDI Science Team, Observations of the diurnal tide from space, *Amer. Meteor. Soc.*, **51**, 3077–3093, 1994.

Hecht, J. H., R. L. Waltersheid, R. G. Roble, R. S. Lieberman, E. R. Talaat, S. K. Ramsay Howat, R. P. Lowe, D. N. Turnbull, C. S. Gardner, R. States, and P. D. Dao, A comparison of atmospheric tides inferred from observations at the mesopause during ALOHA-93 with the model predictions of the TIME-GCM, *J. Geophys. Res.*, **103**, 6307–6321, 1998.

Hitchman, M. H. and C. B. Leovy, Diurnal tide in the equatorial middle atmosphere as seen in LIMS temperatures, *J. Atmos. Sci.*, **42**, 557–561, 1985.

Liebermann, R. S., Nonmigrating diurnal tides in the equatorial middle atmosphere, *J. Atmos. Sci.*, **48**, 1112–1123, 1991.

McLandress, C., Y. Rochon, G. G. Shepherd, B. H. Solheim, G. Thuillier, and F. Vial, The meridional wind component of the thermospheric tide observed by WINDII on UARS, *Geophys. Res. Lett.*, **21**, 2417–2420, 1994.

McLandress, C., G. G. Shepherd, and B. H. Solheim, Satellite observations of thermospheric tides: Results from the Wind Imaging Interferometer on UARS, *J. Geophys. Res.*, **101**, 4093–4114, 1996.

Meek, C. E., A. H. Manson, S. J. Franke, W. Singer, P. Hoffmann, R. R. Clark, T. Tsuda, T. Nakamura, M. Tsutsumi, M. Hagan, D. C. Fritts, J. Isler, and Yu. I. Portnyagin, Global study of northern hemisphere quasi 2-day wave events in the summers of 1992 and 1991, *J. Atmos. Terr. Phys.*, **58**, 1401–1412, 1996.

Meyer, C. K., Gravity wave interactions with mesospheric planetary waves: a mechanism for penetration into the Termosphere-Ionosphere System, submitted to *J. Geophys. Res.*, 1999.

Palo, S. E., M. E. Hagan, C. E. Meek, R. A. Vincent, M. D. Burrage, C. McLandress, S. J. Franke, W. E. Ward, R. R. Clark, P. Hoffmann, R. Johnson, D. Kurschner, A. H. Manson, D. Murphy, T. Nakamura, Yu. I. Portnyagin, J. E. Salah, R. Schminder, W. Singer, T. Tsuda, T. S. Virdi, and Q. Zhou, An intercomparison between the GSWM, UARS, and ground based radar observations: a case-study in January 1993, *Ann. Geophysicae*, **15**, 1123–1141, 1997.

Reber, C. A., C. E. Trevathan, R. J. McNeal, and M. R. Luther, Upper Atmosphere Research Satellite (UARS) mission, *J. Geophys. Res.*, **98**, 10,643–10,647, 1993.

Roble, R. G. and E. C. Ridley, A thermosphere-ionosphere-mesosphere electrodynamics general circulation model (TIME-GCM): Equinox solar cycle minimum simulations (30–500 km), *Geophys. Res. Lett.*, **21**, 417–420, 1994.

Roble, R. G. and G. G. Shepherd, An analysis of wind imaging interferometer observations of $O(^1S)$ equatorial emission rates using the thermosphere-ionosphere-mesosphere-electrodynamics general circulation model, *J. Geophys. Res.*, **102**, 2467–2474, 1997.

Rodger, C. D. and A. J. Prata, Evidence for a travelling two-day wave in the middle atmosphere, *J. Geophys. Res.*, **86**, 9661–9664, 1981.

Shepherd, G. G., G. Thuillier, W. A. Gault, B. H. Solheim, C. Hersom, J. M. Alunni, J.-F. Brun, S. Brune, P. Charlot, L. L. Cogger, D.-L. Desaulnier, W. F. E. Evans, R. L. Gattinger, F. Girod, D. Harvie, R. H. Hum, D. J. W. Kendal, E. L. Llewellin, R. P. Lowe, J. Ohrt, F. Pasternako, O. Peilet, I. Powell, Y. Rochon, W. E. Ward, R. H. Wiens, and J. Wimperis, WINDII, the wind imaging interferometer on the Upper Atmosphere Research Satellite, *J. Geophys. Res.*, **98**, 10,725–10,750, 1993a.

Shepherd, G. G., G. Thuillier, B. H. Solheim, S. Changra, L. L. Cogger, M. L. Duboin, W. F. J. Evans, R. L. Gattinger, W. A. Gault, M. Herse, A. Hauchecorne, C. Lathuilliere, E. J. Llewellyn, R. P. Lowe, H. Teitelbaum, and F. Vial, Latitudinal structure in atomic oxygen concentrations observed with WINDII on UARS, *Geophys. Res. Lett.*, **20**, 1303–1306, 1993b.

Shepherd, G. G., R. G. Roble, S.-P. Zhang, C. McLandress, and R. H. Wiens, Tidal influence on midlatitude airglow: Comparison of satellite and ground-based observations with TIME-GCM predictions, *J. Geophys. Res.*, **103**, 14,741–14,751, 1998.

Shepherd, M. G., A. Dudhia, M. Lopez-Puertas, and W. F. J. Evans, Upper mesosphere temperatures in summer: WINDII observations and comparisons, *Geophys. Res. Lett.*, **24**, 357–360, 1997.

States, R. J. and C. S. Gardner, Influence of the diurnal tide and thermospheric heat sources on the formation of mesospheric temperature inversion layers, *Geophys. Res. Lett.*, **25**, 1483–1486, 1998.

Twomey, S., *Introduction to the Mathematics of Inversion in Remote Sensing and Indirect Measurements*, 243 pp., Development of Geomathematics, 3. Elsevier Scientific Publishing Company, Amsterdam, 1977.

Wang, D. Y., C. McLandress, E. L. Fleming, W. E. Ward, B. Solheim, and G. G. Shepherd, Empirical model of 90–120 km horizontal winds from wind-imaging interferometer green line measurements in 1992–1993, *J. Geophys. Res.*, **24**, 1,127–1,130, 1997.

Ward, W. E., Tidal mechanisms of dynamical influence on oxygen recombination airglow in the mesosphere and lower thermosphere, *Adv. Space Res.*, **21**(6), 795–805, 1998.

Ward, W. E., D. Y. Wang, B. H. Solheim, and G. G. Shepherd, Observations of the two-day wave in WINDII data during January 1993, *Geophys. Res. Lett.*, **23**, 2923–2926, 1996.

Ward, W. E., B. H. Solheim, and G. G. Shepherd, Two day wave induced variations in the oxygen green line volume emission rate: WINDII observations, *Geophys. Res. Lett.*, **24**, 1127–1130, 1997.

Ward, W. E., J. Oberheide, M. Riese, P. Preusse, and D. Offermann, Tidal signatures in temperature data from the CRISTA I mission, *J. Geophys. Res.*, submitted, June, 1998.

Wiens, R., S.-P. Zhang, R. Peterson, and G. Shepherd, Tides in Emission Rate and Temperature from the O_2 Nightglow over Bear Lake Observatory, *Geophys. Res. Lett.*, **22**, 2637–2640, 1995.

Wu, D. L., A study of the diurnal tide and the two-day wave with the High Resolution Doppler Imager (HRDI), Ph.D. Thesis, University of Michigan, 201 pp., 1994.

Wu, D. L., P. B. Hays, W. R. Skinner, A. R. Marshall, M. D. Burrage, R. S. Lieberman, and D. A. Ortland, Observations of the quasi-2-day wave from the High Resolution Doppler Imager on UARS, *Geophys. Res. Lett.*, **20**, 2853–2856, 1993.

Wu, D. L., P. B. Hays, and W. R. Skinner, A least squares method for spectral analysis of space-time series, *J. Atmos. Sci.*, **52**, 3501–3511, 1995.

Wu, D. L., E. F. Fishbein, W. G. Read, and J. W. Waters, Excitation and evolution of the quasi-2-day wave observed in UARS/MLS temperature measurements, *J. Atmos. Sci.*, **53**, 728–738, 1996.

Yu, J., R. States, S. J. Franke, C. S. Gardner, and M. Hagan, Observations of tidal temperature and wind perturbations in the mesopause region above Urbana, IL (40°N, 88°W), *Geophys. Res. Lett.*, **24**, 1207–1210, 1997.

Yudin, V. A., B. V. Khattatov, M. A. Geller, D. A. Ortland, C. McLandress, and G. G. Shepherd, Thermal tides and studies to tune the mechanistic tidal model using UARS observations, *Ann. Geophysicae*, **15**, 1205–1220, 1997.

Zhang, S. P., R. H. Wiens, B. H. Solheim, and G. G. Shepherd, Nightglow zenith emission rate variations in $O(^1S)$ at low latitudes from WINDII observations, *J. Geophys. Res.*, **103**, 6251–6259, 1998.

M. G. Shepherd (e-mail: marianna@windii.yorku.ca), W. E. Ward, B. Prawirosoehardjo, R. G. Roble, S.-P. Zhang, and D. Y. Wang